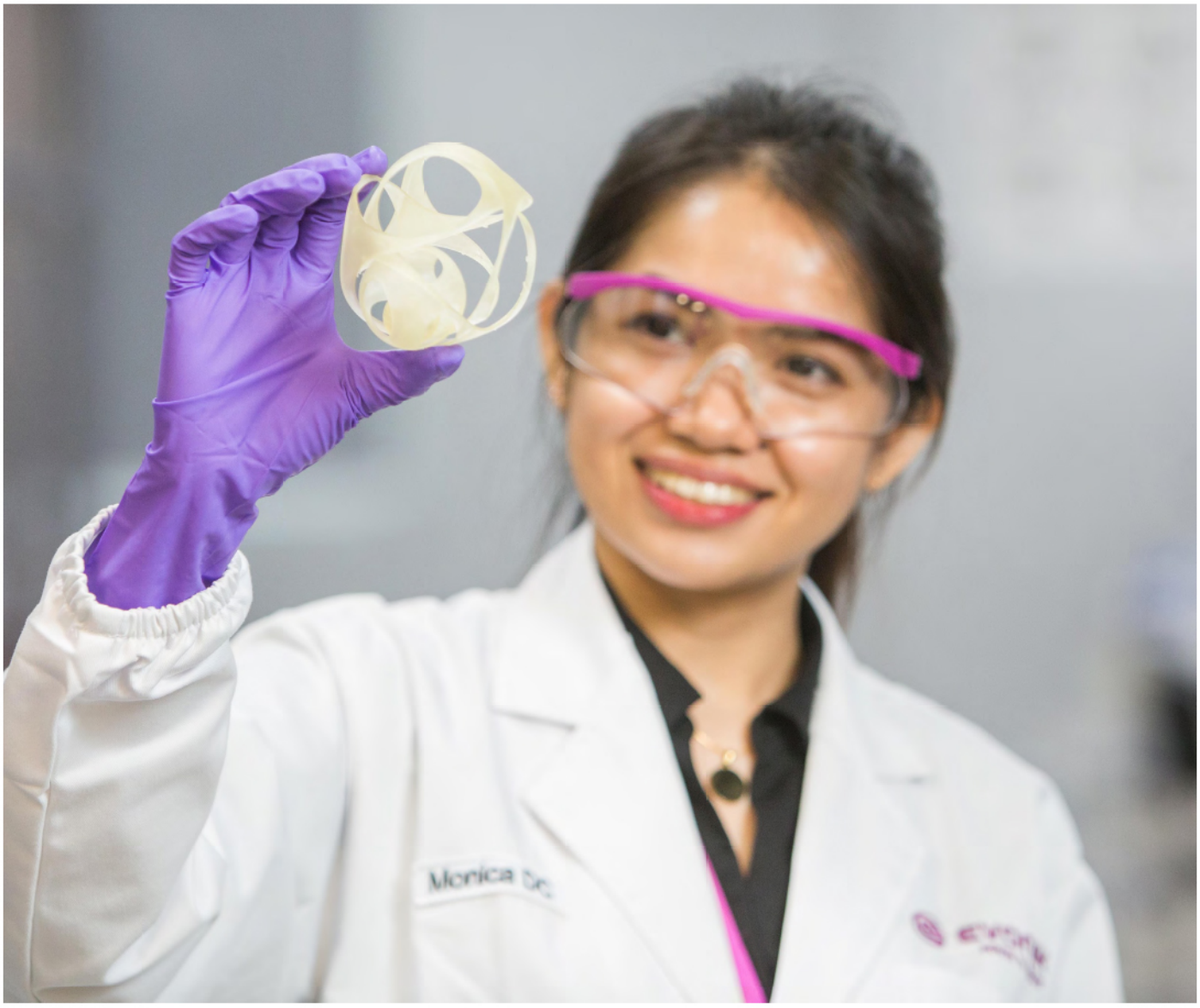

# Pushing the boundaries of chemistry? It takes #HumanChemistry

Make your curiosity and talent as a chemist matter to the world with a specialty chemicals leader. Together, we combine cutting-edge science with engineering expertise to create solutions that answer real-world problems. Find out how our approach to technology creates more opportunities for growth, and see what chemistry can do for you at:

**evonik.com/career**

EVONIK
Leading Beyond Chemistry

ADVANCED FUNCTIONAL MATERIALS
www.afm-journal.de

# Photodoping and Fast Charge Extraction in Ionic Carbon Nitride Photoanodes

*Christiane Adler, Shababa Selim, Igor Krivtsov, Chunyu Li, Dariusz Mitoraj, Benjamin Dietzek, James R. Durrant,* and Radim Beranek**

**Ionic carbon nitrides based on poly(heptazine imides) (PHI) represent a vigorously studied class of materials with possible applications in photocatalysis and energy storage. Herein, for the first time, the photogenerated charge dynamics in highly stable and binder-free PHI photoanodes using in operando transient photocurrents and spectroelectrochemical photoinduced absorption measurements is studied. It is discovered that light-induced accumulation of long-lived trapped electrons within the PHI film leads to effective photodoping of the PHI film, resulting in a significant improvement of photocurrent response due to more efficient electron transport. While photodoping is previously reported for various semiconductors, it has not been shown before for carbon nitride materials. Furthermore, it is found that the extraction kinetics of untrapped electrons are remarkably fast in these PHI photoanodes, with electron extraction times (ms) comparable to those measured for commonly employed metal oxide semiconductors. These results shed light on the excellent performance of PHI photoanodes in alcohol photoreforming, including very negative photocurrent onset, outstanding fill factor, and the possibility to operate under zero-bias conditions. More generally, the here reported photodoping effect and fast electron extraction in PHI photoanodes establish a strong rationale for the use of PHI films in various applications, such as bias-free photoelectrochemistry or photobatteries.**

## 1. Introduction

Polymeric carbon nitride (PCN) materials represent one of the most vigorously studied classes of low-cost, tunable, and highly stable polymeric photocatalysts, with potential applications in light-driven hydrogen production, selective oxidations of organic substrates, and other useful chemical transformations.[1] The fundamental photophysical properties and processes (photoexcitation, recombination, charge separation, photoluminescence) that govern the performance of PCN-based photocatalysts have been intensely studied,[2] revealing many aspects related to the electron transfer within and between different PCN units,[2f] charge separation,[2a,b] and recombination[2c] processes, in addition to providing insight into the hole transfer to electron donors.[2e]

Recently, there has been increasing interest in poly(heptazine imide) (PHI)-based materials, a class of (semi)crystalline ionic PCNs comprising stacks of 2D heptazine-based networks and alkali metal cations and/or protons.[1a,3] Compared to conventional PCN materials, the PHI photocatalysts often exhibited higher photocatalytic activity owing to their surface functional (e.g., cyanamide) groups and thus improved dispersibility.[1a,3,4] Moreover, it has been demonstrated that the photogenerated electrons trapped within PHI materials can be effectively accumulated and stored,[2h,5] in order to be later utilized, for example, for hydrogen evolution in the dark upon addition

C. Adler, I. Krivtsov, D. Mitoraj, R. Beranek
Institute of Electrochemistry Ulm University
Albert-Einstein-Allee 47, 89081 Ulm, Germany
E-mail: radim.beranek@uni-ulm.de

S. Selim, J. R. Durrant
Department of Chemistry and Centre for Processable Electronics
MSRH
Imperial College London
White City Campus, London W12 0BZ, UK
E-mail: j.durrant@imperial.ac.uk

The ORCID identification number(s) for the author(s) of this article can be found under https://doi.org/10.1002/adfm.202105369.



**DOI: 10.1002/adfm.202105369**

C. Li, B. Dietzek
Department Functional Interfaces
Leibniz Institute of Photonic Technology Jena (IPHT)
Albert-Einstein-Straße 9, 07745 Jena, Germany

C. Li, B. Dietzek
Institute of Physical Chemistry
Friedrich-Schiller University Jena
Helmholtzweg 4, 07743 Jena, Germany

B. Dietzek
Centre for Energy and Environmental Chemistry Jena (CEEC Jena)
Friedrich-Schiller University Jena
Philosophenweg 7a, 07743 Jena, Germany

of a cocatalyst,[6] or in solar batteries.[5b] While some studies have suggested that structural defects (e.g., cyanamide moieties) can be beneficial for photocatalytic activity,[2g,i,4b,6b] the presence of deep electron traps and resulting electron accumulation and faster recombination have been typically identified as the principal bottleneck in efficient operation of both PHI-based and conventional PCN photocatalysts.[2c,d,g,h]

Most research to date on the fundamental photophysics of PCN-based materials has been carried out using powder suspensions, since the fabrication of stable PCN-based photoelectrodes is very challenging, mainly due to the poor adhesion of PCN to conductive substrates[5b,7] and the poor conductivity of PCN films, hindering efficient charge extraction into the external circuit.[8] Therefore, the very scarce spectroscopic studies of conventional PCN photoelectrodes have been typically carried out using binders such as Nafion or $TiO_2$ electron-transport layers,[2a,9] which can complicate understanding of the observed behavior. To the best of our knowledge, there are no reports available on fundamental photophysical properties of photoelectrodes based on ionic carbon nitrides (PHI).

We have recently reported a novel method for fabrication of thin, binder-free (≈400–500 nm) PHI photoanodes exhibiting excellent long-term mechanical and photoelectrochemical stability.[10] The synthetic process capitalizes on the use of small (≈10 nm) nanoparticles of alkali metal-containing poly(heptazine imide) (K,Na-PHI),[4a] which are fully soluble in water and enable an easy sol–gel processing, yielding highly stable PHI films on various substrates including FTO.[10] Our PHI photoanodes exhibited selective (≈100% Faradaic efficiency) photoelectrocatalytic conversion of various alcohols, standing out, in particular, by their very low photocurrent onset potential and exceptionally high fill factor, thus permitting effective photoreforming of alcohols to hydrogen even without any applied electric bias.[10]

Herein, we provide, for the first time, in operando investigations of photoelectrochemical processes in the highly stable, binder-free PHI photoanodes. We employ transient photocurrent (TPC) and spectroelectrochemical photoinduced absorption spectroscopy measurements that enable us to directly observe photogenerated charge dynamics under operando conditions and correlate these with the concomitantly measured photocurrent. This allows us to observe the impact of charge accumulation within our PHI photoanodes on photocurrent generation from methanol oxidation. We have previously employed these techniques to study photoelectrochemical processes in various metal oxide photoelectrodes.[11] Interestingly, we find that the excellent performance of the PHI photoanodes originates, at least in part, from fast electron extraction on a timescale similar to that observed for commonly employed inorganic photoanodes ($TiO_2$, $WO_3$, $BiVO_4$). Furthermore, our findings suggest that extensive electron trapping and accumulation results in effective photodoping in PHI photoanodes, which leads to enhanced electron transport, improving thus the photoelectrocatalytic activity. While photodoping effects upon light-induced electron accumulation have been previously reported for various inorganic[12] and organic semiconductors,[13] we demonstrate for the first time that photodoping can be operative also in photoelectrodes based on ionic carbon nitrides.

## 2. Results and Discussion

The sol–gel processing of water-soluble K,Na-PHI yields thin (≈400–500 nm) and porous PHI films on FTO glass that are easily permeable by the electrolyte. The structural, optical, and photoelectrochemical properties of our porous PHI photoanodes (PHI-DB/S450) were reported in detail by Adler et al.[10] While the PHI photoanodes did not oxidize water, the photocurrents during oxidation of alcohols, such as methanol, were among the highest observed for PCN-based photoanodes. This is exemplified in **Figure 1**a, which also shows the exceptionally high fill factor of the *J*–*V* curve, across a wide potential range. This feature is reminiscent of the behavior of mesoporous inorganic photoanodes, such as $TiO_2$.[14] In addition, the PHI photoanodes outperform all PCN-based photoanodes and even

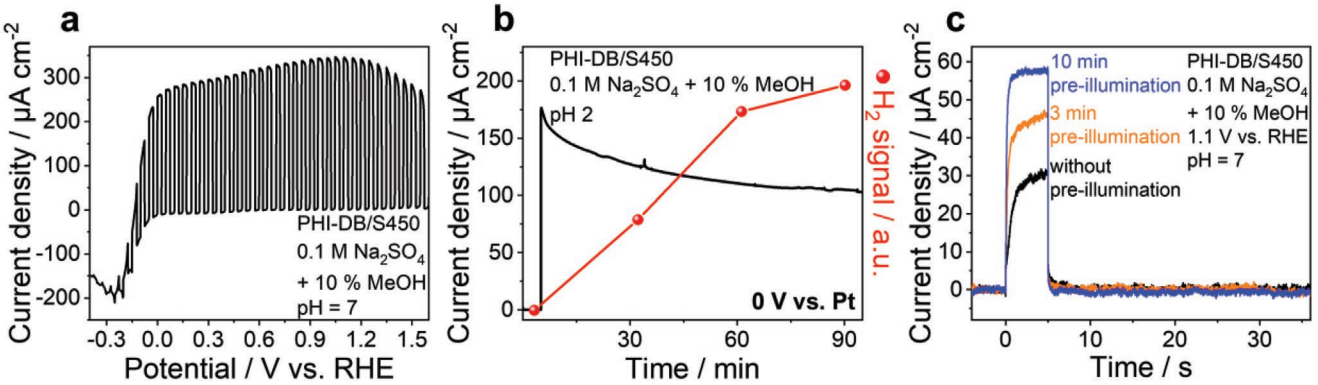


**Figure 1.** Photoelectrochemical characteristics of PHI carbon nitride photoanodes for methanol oxidation. a) LSV curves (scanned in cathodic direction with a sweep-rate of 5 mV $s^{-1}$) of PHI-DB/S450 in 0.1 M $Na_2SO_4$ with 10 v% methanol (pH 7.0) upon on/off illumination (2 sun, 5 s light/5 s dark) from back side. b) Bias-free photoreforming of methanol: photocurrent (black) and $H_2$ evolution (red) detected by the GC-BID for PHI-DB/S450 in a two-electrode setup (0 V vs Pt counter electrode; 1 sun illumination; 0.1 M $Na_2SO_4$ with 10% v/v methanol; for this experiment the pH was adjusted with $H_2SO_4$ to pH 2 in order to decrease the ohmic drop in the electrolyte). c) Photocurrent transients measured of PHI-DB/S450 in 0.1 M $Na_2SO_4$ + 10 v% methanol at 1.1 V versus RHE without (black), with 3 min (amber) or 10 min (blue) preillumination directly before measurement. Excitation with 365 nm LED (5 mW $cm^{-2}$) for 5 s and dark for 45 s.

most inorganic semiconductors in terms of the very negative photocurrent onset potential (below 0 V vs RHE). This allows for effective photoreforming of methanol to hydrogen even under bias-free conditions (Figure 1b), which is—to the best of our knowledge—unprecedented behavior for any "soft matter" photoanodes based on organic polymers. Note that bias-free photoreforming of methanol to hydrogen and formaldehyde is thermodynamically an endergonic ($\Delta_r G^{\circ}_{298K}$ = +63.7 kJ mol$^{-1}$) reaction,[15] hence nominally a truly photosynthetic conversion.[16] In addition, the absence of the photocurrent spikes which are a typical fingerprint of (sub)surface recombination[17] in the linear sweep voltammogram (LSV) of the PHI-DB/S450 film even at potentials down to 0 V versus RHE indicates the negligible surface recombination losses at the PHI–electrolyte interface (Figure 1a).[11a,18]

Photocurrent transients measured for the PHI photoanodes when illuminated by an LED pulse for 5 s (365 nm LED, 5 mW cm$^{-2}$) allow us to study the effect of the preillumination on the observed photocurrents for methanol oxidation, as shown in Figure 1c. We do this by preilluminating the sample under applied potential (1.1 V vs RHE) with continuous LED irradiation (also 365 nm, 5 mW cm$^{-2}$) in the presence of methanol, prior to measuring the photocurrent transient with the LED pulse. From Figure 1c, we observe that preillumination not only leads to a direct enhancement in the obtained photocurrents, but also affects the speed of saturation of the photocurrent. Photocurrent saturation (plateau) implies that the system has reached steady-state conditions, whereby the surface concentration of photogenerated holes is not changing and the flux of photogenerated holes into the surface is balanced by the flux of holes across the interface contributing to the photocurrent (i.e., rate of methanol oxidation) and by the flux of holes due to (surface or subsurface) recombination. We point out that the so-called photocurrent doubling effect can be ruled out in our case since the half-wave oxidation potential of hydroxymethyl radical (the product of one-electron oxidation of methanol) is ≈–0.32 V versus RHE, which makes the injection of an electron from the radical to the conduction band edge of PHI-DB/S450 (–0.63 V vs RHE) rather unlikely.[10] Our pulsed LED-induced photocurrent transients (Figure 1c) suggest that a preillumination time of ≈10 min is sufficient for the system to reach optimum performance. This was further confirmed from measurement of the photocurrents during preillumination using chronoamperometry (Figure S1, Supporting Information), where we can observe that the photocurrent continues to increase and plateaus within a period of 7–10 min of preillumination. Intriguingly, the slow rise of the photocurrent transient without preillumination (Figure 1c, black trace), most likely related to the typically poor intrinsic conductivity of PCN materials, accelerates significantly with prolonged preillumination of the system (Figure 1c, blue trace). This behavior has some similarity to photodoping effects reported previously for various inorganic[12] and organic[13] semiconductors, as we discuss further later.

Next, we employ photoinduced absorption (PIA) spectroscopy as an operando probe of accumulation of charges in our PHI photoanodes under the same pulsed LED irradiation employed for the photocurrent transients shown in Figure 1c, with/without preillumination. The PIA spectra of our PHI photoanodes shown in **Figure 2**a present a relatively broad spectral feature across the visible region probed herein (460–800 nm), with a maximum at ≈600 nm when recorded without any preillumination (black trace). No change in the magnitude of the optical signals is observed when illuminating with a higher light intensity LED pulse (green trace, 10 mW cm$^{-2}$). The differential optical density signal diminishes significantly upon preillumination (blue trace) leaving a flat featureless spectrum across the probed region. Furthermore, the loss of the optical signal in the absence of methanol (red trace), which effectively scavenges the photogenerated holes at the surface,[2e] indicates that the observed signals are likely to be related to photogenerated electrons.

Figure 2b plots the kinetics of the PIA signal at 650 nm induced by pulsed LED irradiation without preillumination, with/without methanol. When the LED pulse is turned off,

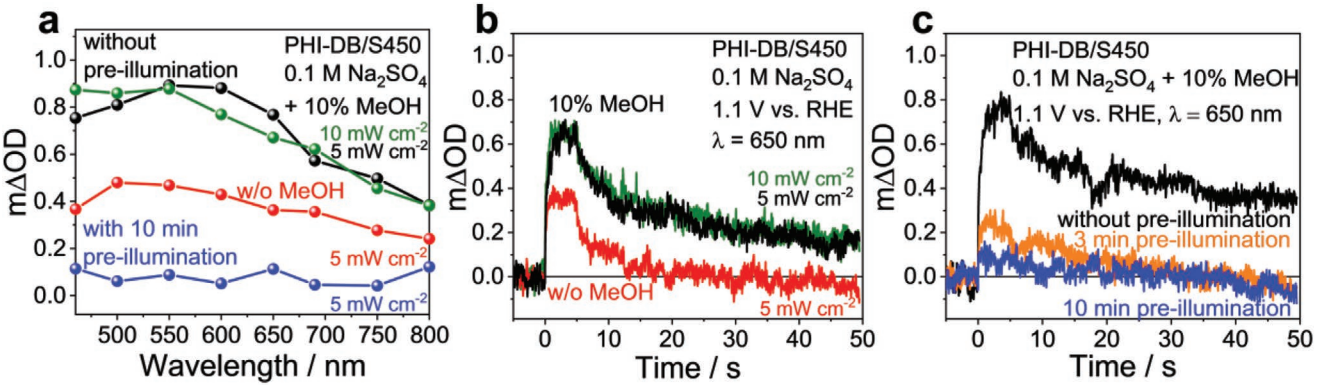


**Figure 2.** Spectroelectrochemical characteristics of PHI carbon nitride photoanodes with and without preillumination. a) Comparison of PIA spectra with 365 nm LED excitation (5 mW cm$^{-2}$ (black) and 10 mW cm$^{-2}$ (green)) without any preillumination, and with a 10 min preillumination (blue), measured in 0.1 M $Na_2SO_4$ with 10 v% MeOH. Spectrum obtained without preillumination in absence of any MeOH is also shown (red). b) PIA optical trace and decay monitored at $\lambda$ = 650 nm for PHI-DB/S450 photoanodes in absence of any preillumination, when excited with 365 nm LED (5 mw cm$^{-2}$ (black) and 10 mW cm$^{-2}$ (green) in 0.1 M $Na_2SO_4$, with 10 v% MeOH. Analogous measurement in absence of any MeOH is also shown (red). The samples were excited with an LED pulse for 5 s and subsequently left in the dark for 45 s during the measurement. c) PIA of PHI-DB/S450 in 0.1 M $Na_2SO_4$ + 10 v% MeOH without (black), with 3 min (amber) or 10 min (blue) preillumination directly before measurement at 650 nm. Excitation with 365 nm LED (5 mW cm$^{-2}$) for 5 s and left in dark for 45 s. All measurements were obtained at 1.1 V versus RHE.

the PIA signal decays very slowly in the presence of methanol ($t_{50\%} \approx$ 20–30 s). A faster decay of the PIA signal is observed in the absence of methanol, attributed to the absence of methanol resulting in unreacted photogenerated holes recombining with accumulated electrons, and further supporting our assignment of the PIA signal to electrons. In contrast to these slow PIA decays, the concomitant transient photocurrent measurements (Figure 1c) show a rapid drop in the photocurrent to zero when the LED is switched off. The slow nature of the optical signal decay, consistent with previous reports of carbon nitrides,[2c,d,h,5b,6b] indicates this signal originates primarily from relatively immobile and therefore deeply trapped, electrons. Furthermore, consistent with the *J–V* characteristics (Figure 1a), the magnitude of the optical signal and the photocurrents in the absence of preillumination are observed to be largely independent of the applied bias (Figure S2, Supporting Information). This is in agreement with the very good fill factor of our PHI films indicating that the applied potential has only a minor effect on the charge accumulation and extraction properties of the photoanode (Figure 1a).

We now employ PIA to investigate the effect of preillumination on the accumulation of photogenerated electrons, shown in Figure 2c. Upon preillumination, there is a considerable loss in the magnitude of PIA signal at 650 nm, combined with an acceleration of its decay kinetics. In addition, as shown in Figure S3 of the Supporting Information, increasing the light intensity from 5 to 10 mW $cm^{-2}$ for both the preillumination steps and the subsequent PIA/photocurrent transients results in the following effects: i) an increase in the photocurrent density, ii) earlier stabilization of the photocurrent density within 3 min of preillumination (vs ≈10 min for 5 mW $cm^{-2}$), correlated with iii) a concomitant earlier decrease in the optical signal (by 3 min). Critically, the magnitude of the PIA signal without preillumination (assigned above to photoinduced trapped electrons) is also found to be unaffected by the light intensity (Figure 2b; Figure S3, Supporting Information). We propose that this behavior is related to the gradual filling of trap states by photogenerated electrons during illumination, resulting in significant electron accumulation within the film. Further, the data also indicates the requirement for a critical threshold of electron accumulation that leads to optimal performance in this system. We assume that the observed electron accumulation corresponds to the formation of $PHI^{\bullet-}$ anion radicals known to occur in ionic PHI-type materials.[2c,h,3a,5,6b] These accumulated electrons are only slowly scavenged by oxygen in the dark,[2h] and exhibit long carrier lifetimes (>30 s, Figure 2b,c) when surface holes have been scavenged by methanol, highlighting the unreactive nature of these trapped charges (Figure 2a,b). Such $PHI^{\bullet-}$ anion radicals can also be generated electrochemically[5b] by applying a negative potential to the PHI electrode. Indeed, one can observe that at the potential range of –0.4 to –0.9 V versus RHE the transmittance of the film at 650 nm is decreased, corroborating the assumption that the absorbance increase in the visible range observed in the PIA experiments is due to reduced PHI species (Figure S4, Supporting Information). On the other hand, it was previously reported that accumulated electrons in ionic PCNs can be utilized for hydrogen evolution in the presence of a cocatalyst.[2g,6] The fact that electron trapping and accumulation in our PHI photoanodes does not impair but rather improves their photoelectrocatalytic performance is rather intriguing, especially in view of previous reports on the detrimental effects of electron trapping on the performance of PCN-based photocatalysts.[2c,d,g] For example, our previous spectroscopic investigations of ionic-type PCN in form of particle suspensions have demonstrated accelerated recombination upon accumulation of long-lived, trapped electrons.[2c] In order to investigate this further, we applied nanosecond-transient absorption (ns-TA) spectroscopy under bias-free conditions to investigate the charge kinetics of the PHI-DB/S450 films on a timescale of 50 ns to 5 µs in the presence of air, water, and methanol (see Note S1, Supporting Information). We observe a faster decay of the optical signal in the presence of methanol, consistent with enhanced recombination resulting from more electrons accumulation in the material in the presence of effective hole scavenger (Figure S5, Supporting Information), in line with our previous results.[2c] However, such negative effects of electron accumulation in our PHI-DB/S450 photoanodes are clearly outbalanced by the positive effect of trap passivation, as evidenced by enhanced photocurrent generation (Figure 1c), which is superior to that typically encountered in conventional (non-ionic) PCN materials. In this context, we speculate that, due to the distinct nature of the ionic PHI-based materials and the highly porous nature of our PHI-DB/S450 photoanodes[10] (as compared to a dense analogue that shows much lower photocurrents, Figure S6, Supporting Information), the negative charge of the accumulated trapped electrons in the PHI photoanodes can be effectively screened by cations ($K^+$, $Na^+$, $H^+$) from the film and from the solution, which may at least partially eliminate the detrimental effects of charge accumulation. We find that electron accumulation during preillumination is reversible, shown in Figure S7 of the Supporting Information. The loss in the optical signal (i.e., due to electron accumulation) resulting from repeated preillumination cycles (blue trace) is recovered to the initial optical trace observed prior to any preillumination when the sample has been left in the dark over a period of 24 h (black trace). This reversible behavior demonstrates that our photoanodes are not suffering oxidation or degradation. Rather, the loss in the optical signal and the concomitant increase in the photocurrent is attributed to the filling of trap states with long-lived unreactive charge carriers.

Our results indicate that long lived electron accumulation in our PHI photoanodes is correlated with a significant increase of the overall photocurrent, assigned to trap filling. This beneficial effect of electron accumulation can be understood as resulting from an effective photodoping of the PHI film, an effect that has been observed for a range of inorganic[12] and organic[13] semiconductors, however not reported previously for PCN materials. The photodoping during preillumination effectively fills/passivates deep electron traps and improves the charge transport through the film, as is also indicated by significantly lower impedance of the electrode upon illumination (Figure S8, Supporting Information). In relatively disordered organic materials like our PHI films, the electron transport mechanism can be typically understood in terms of a thermally activated hopping of electrons that are relatively localized in shallow trap states.[19] Upon effective filling of deep trap states during preillumination (i.e., by photodoping), the electron trapping

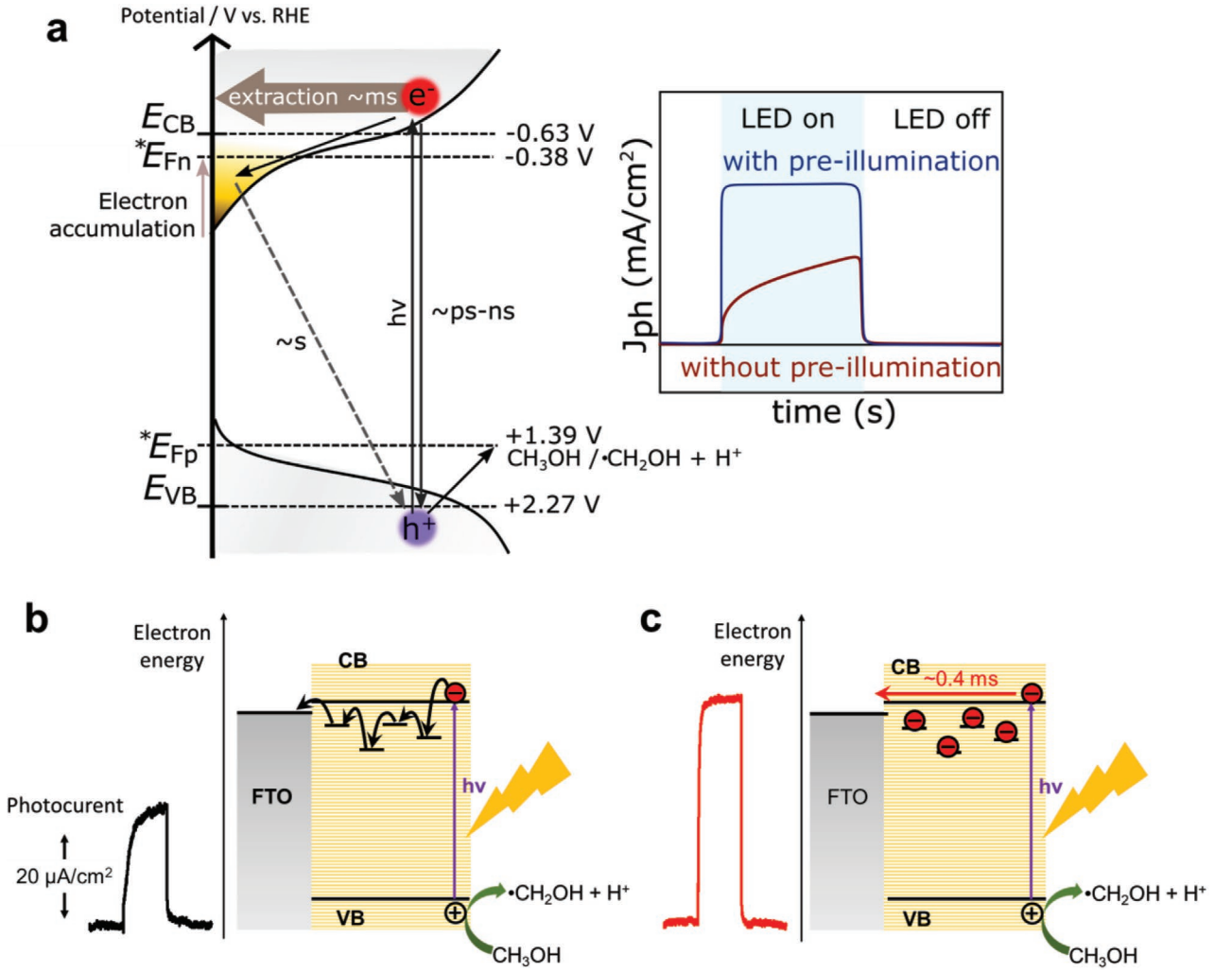


**Scheme 1.** Schematic illustration of processes governing the photocurrent generation in porous PHI films. a) The accumulation of long-lived (>30 s) electrons in trap states occurs within s-mins and leads to effective photodoping of the PHI film, which enables very fast (≈0.4 ms) electron extraction from the PHI film into the FTO electrode and improves significantly the photocurrent response. $E_{VB}$, $E_{CB}$, $^*E_{Fn}$, and $^*E_{Fp}$ stand for the valence band edge, the conduction band edge, and the quasi-Fermi level of electrons and holes under illumination, respectively, and have been determined previously.[10] The effect of photodoping on the electron transport through the PHI film. b) In the absence of photodoping, a significant proportion of photogenerated electrons undergo deep charge trapping, impeding the efficiency and kinetics of electron extraction to the external circuit. c) In the presence of photodoping resulting in the filling/passivation of trap states, electron extraction becomes more efficient. All recombination pathways are omitted for the sake of clarity.

is avoided and the electron transport through the PHI film is effectively enhanced (**Scheme 1**b,c), as we investigate in more detail below. From the chemical point of view, the transformations which the PHI film undergoes upon photodoping can be well rationalized considering the charge-stabilizing effect of its surface functional groups (Figure S9, Supporting Information). The role of the cyanamide moieties in the stabilization of the $PHI^{•-}$ is well established.[2c,5a,6b] Therefore, we hypothesize that initially upon irradiation in the presence of an electron donor (MeOH) the formed $PHI^{•-}$ anion radical is delocalized over the heptazine units (Figure S9(1),(2), Supporting Information). The stability of the radical is ensured by the negative charge on the deprotonated cyanamide species, which impedes its fast discharge. The coupled effect of the accumulated electrons and protons abstracted from MeOH leads to the formation of the reduced form of the terminal PHI heptazine moieties followed by the rearrangement of the conjugation in the system and resulting in neutralization of the negative charge on the cyanamide species (Figure S9(3), Supporting Information). Thus, the PHI film reaches the photodoped state in which the transport of the negative charge is improved. The return of the PHI film from the photodoped to the initial non-photodoped state might be accomplished, for example, via its gradual reaction with atmospheric $O_2$ in the dark leading to the conjugation change and stabilization of the negative charge on the cyanamide group (Figure S9(4), Supporting Information). Furthermore, we assume that also cyamelurate groups bearing a deprotonated $C{-}O^-$ function that are also present in our PHI material[4a] may act in a similar manner to the cyanamide moieties in the stabilization of the $PHI^{•-}$ anion radicals.

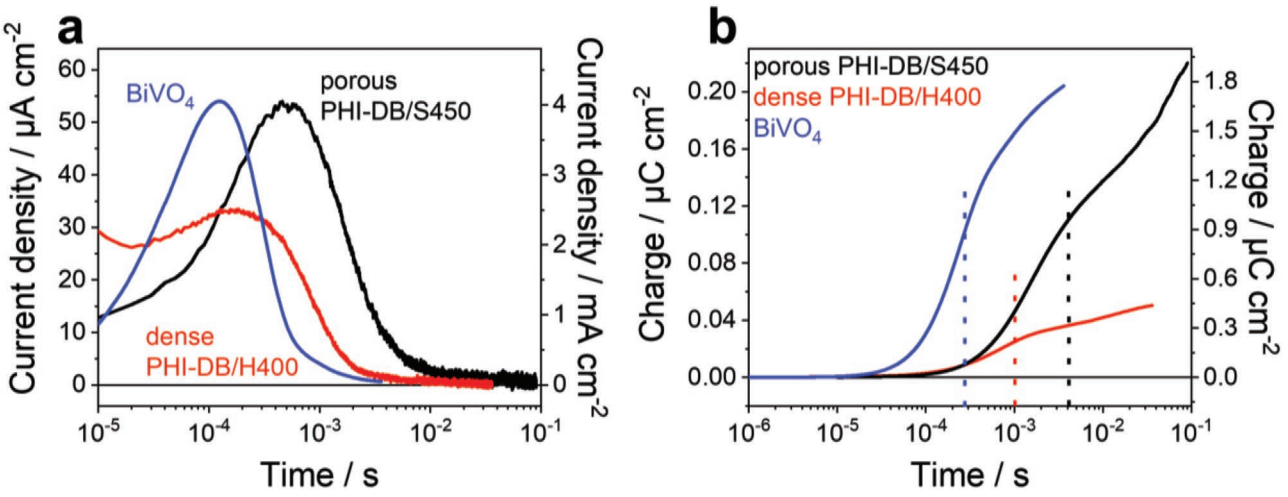


**Figure 3.** Charge extraction characteristics of PHI carbon nitride photoanodes. a) Transient photocurrents (TPC) and b) integrated TPCs showing the total charges extracted from porous PHI-DB/S450 (black) and dense PHI-DB/H400 (red) photoanodes in 0.1 M $Na_2SO_4$ + 10 v% MeOH. The samples were excited from the back with a 355 nm pulsed laser (7 ns pulse width, excitation density of 300 μJ $cm^{-2}$) at 1.1 V versus RHE. For comparison with typical metal oxides, TPC (right axis) for a dense $BiVO_4$ photoelectrode (of thickness 400–250 nm) in 0.1 M KP buffer for front side excitation with a 355 nm pulsed laser at 1.23 V versus RHE is shown.

We now turn to the electron extraction kinetics of our PHI photoanodes using TPC measurements employing short pulse (ns) laser photoexcitation (**Figure 3**). We compare the charge extraction transients of our porous PHI photoanode (PHI-DB/S450) with a dense (i.e., nonporous) analogue (PHI-DB/H400).[10] The dense film, although having similar thicknesses (≈400–500 nm) and nearly the same intrinsic structural and physicochemical properties as PHI-DB/S450, has much lower photoelectrocatalytic activity and did not show any notable effect of preillumination (Figure S6, Supporting Information), attributed to its lower surface area and correspondingly lower ability to accumulate charges.[10] The timescale of the TPC maxima (Figure 3a), which represents the highest rate of electron extraction, are ≈0.4 ms for porous (PHI-DB/S450) and ≈0.2 ms for dense (PHI-DB/H400) photoanodes. The faster electron extraction times observed for dense compared to porous PHI films is consistent with the different morphologies of the samples, since the electrons in the dense film are extracted via direct path to the back contact, whereas the effective pathlength to the back contact is longer in the porous PHI layer. As these TPC transients employ relatively intense laser pulses (300 $\mu$J $cm^{-2}$, 0.8 Hz repetition rate), it is likely they induce significant trap filling/photodoping. This supposition is supported by the only minor dependence of the TPC kinetics with and without background light bias (LED, 5 mW $cm^{-2}$), shown in Figure S10 of the Supporting Information. The integrated current densities obtained from these TPC measurements show a much higher yield of total charge extracted for the porous photoelectrode in comparison to the dense analogue (Figure 3b), consistent with the corresponding steady-state *J–V* performance (Figure S6, Supporting Information). This is attributed to more efficient methanol oxidation by photogenerated holes due to the higher active surface area of the porous film. The half-time for charge extraction ($t_{50\%}$ rise time in Figure 3b) for the dense (PHI-DB/H400) film is 1 ms, which is faster than 4 ms observed for the porous one (dot line, Figure 3b), attributed to the differences in film morphology discussed above. Interestingly, the charge extraction time is very similar for back or front side irradiation for both samples (Figure S11, Supporting Information), which can be explained by the large optical penetration depth of the laser beam (≈250 and 350 nm for PHI-DB/S450 and PHI-DB/H400, respectively).[10] Remarkably, the timescale (ms) of electron extraction for our PHI photoelectrodes is on the same order of magnitude as bismuth vanadate ($BiVO_4$) photoanodes of comparable thickness,[20] one of the best-performing metal oxide photoanode materials for water oxidation to date.

A schematic representation of electron dynamics within the porous PHI film is shown in Scheme 1. From the data herein, it is apparent that the PHI films exhibit significant trapping of photogenerated electrons in deep trap states, giving rise to long-lived (≈30 s) trapped electrons. Under prolonged (>1 s) irradiation, these trap states become filled with electrons. This results in passivation of these trap states, effectively photodoping the material and improving the efficiency of electron extraction to the external circuit and enhancing photoelectrochemical performance. This photodoping at least partially mitigates the negative impact of the presence of deep trap states in these photoanodes. Remarkably fast (ms) electron extraction kinetics are observed for such a disordered material, assigned to electrons which avoid deep trapping, and consistent with the excellent fill factor of the PHI photoanodes (Figure 1a). On the other hand, without any effective hole scavenger, such as the methanol employed herein, recombination of trapped electrons and VB holes occurs on the seconds timescale (see Figure 2b, red trace), preventing significant water oxidation and resulting in negligible photocurrent densities in the absence of methanol (Figure S12, Supporting Information). Enhancing the kinetics and efficiency of water oxidation by, for example, deposition of cocatalysts[21] would be essential to extend the use of PHI photoanodes from photoelectrocatalytic alcohol conversions to overall water splitting.

## 3. Conclusion

We have studied, for the first time, the photogenerated charge dynamics in stable and binder-free ionic (PHI) carbon nitride photoanodes using TPCs and in operando spectroelectrochemical PIA measurements. Consistent with previous reports,[2c,d,g,h] we observe prolonged irradiation results in electron accumulation in long-lived trap states within the PHI film during illumination. While it is well-established that the electrons trapped in PHI can be utilized for subsequent redox transformations,[2h,5] we demonstrate, for the first time, that the electrons accumulated in the PHI film during illumination passivate deep trap states and thus also effectively photodope the PHI film. This photodoping effect leads to a significant improvement of photocurrent response due to more efficient electron transport. Recombination of trapped electrons with photogenerated holes is suppressed when the hole transfer reaction is fast (e.g., in methanol oxidation). By contrast, the slower and kinetically more challenging hole reactions (e.g., water oxidation) are outcompeted by recombination. While photodoping has been previously reported for various inorganic[12] and organic materials,[13] the here reported beneficial photodoping effect has not been shown before for polymeric carbon nitrides. Moreover, we demonstrate that electrons which avoid deep trapping in these PHI photoanodes exhibit fast (ms) extraction kinetics, with electron extraction times comparable to those measured for commonly employed metal oxide semiconductors (e.g., $TiO_2$, $WO_3$, $BiVO_4$). These results shed light on the excellent performance of PHI photoanodes in alcohol photoreforming, including very negative photocurrent onset, outstanding fill factor, and the possibility to carry out photoreforming under zero-bias conditions.[10] More generally, the here reported photodoping effect and fast electron extraction in PHI photoanodes represent yet another intriguing property of the ionic (PHI-based) carbon nitride materials, and establish a strong rationale for the use of PHI films in various applications, such as bias-free photoelectrochemistry or photobatteries.[5b,c]

## Supporting Information

Supporting Information is available from the Wiley Online Library or from the author.

## Acknowledgements

C.A. and S.S. contributed equally to this work. This work was funded by the Deutsche Forschungsgemeinschaft (DFG, German Research Foundation)—Projektnummer BE 5102/5-1 and 364549901—TRR 234 CataLight [Project B6]. I.K. acknowledges the support of the Alexander von Humboldt Foundation through the Humboldt Research Fellowship. S.S. acknowledges funding from European Union's Horizon 2020 (SUN2CHEM, Grant Agreement No. 884444).

Open access funding enabled and organized by Projekt DEAL.

## Conflict of Interest

The authors declare no conflict of interest.

## Data Availability Statement

The data that support the findings of this study are available from the corresponding author upon reasonable request.

## Keywords

bias-free photoelectrochemistry, carbon nitride, charge extraction, photoanode, photodoping

Received: June 4, 2021
Revised: July 12, 2021
Published online: August 7, 2021

[1] a) A. Savateev, M. Antonietti, *ACS Catal.* **2018**, *8*, 9790; b) A. Savateev, M. Antonietti, *ChemCatChem* **2019**, *11*, 6166; c) X. Wang, S. Blechert, M. Antonietti, *ACS Catal.* **2012**, *2*, 1596; d) X. Wang, K. Maeda, A. Thomas, K. Takanabe, G. Xin, J. M. Carlsson, K. Domen, M. Antonietti, *Nat. Mater.* **2009**, *8*, 76.

[2] a) C. Ye, J.-X. Li, Z.-J. Li, X.-B. Li, X.-B. Fan, L.-P. Zhang, B. Chen, C.-H. Tung, L.-Z. Wu, *ACS Catal.* **2015**, *5*, 6973; b) H. Zhang, Y. Chen, R. Lu, R. Li, A. Yu, *Phys. Chem. Chem. Phys.* **2016**, *18*, 14904; c) W. Yang, R. Godin, H. Kasap, B. Moss, Y. Dong, S. A. J. Hillman, L. Steier, E. Reisner, J. R. Durrant, *J. Am. Chem. Soc.* **2019**, *141*, 11219; d) R. Godin, Y. Wang, M. A. Zwijnenburg, J. Tang, J. R. Durrant, *J. Am. Chem. Soc.* **2017**, *139*, 5216; e) Z. Chen, Q. Zhang, Y. Luo, *Angew. Chem., Int. Ed.* **2018**, *57*, 5320; f) K. L. Corp, C. W. Schlenker, *J. Am. Chem. Soc.* **2017**, *139*, 7904; g) H. Kasap, C. A. Caputo, B. C. Martindale, R. Godin, V. W. Lau, B. V. Lotsch, J. R. Durrant, E. Reisner, *J. Am. Chem. Soc.* **2016**, *138*, 9183; h) C. Li, E. Hofmeister, I. Krivtsov, D. Mitoraj, C. Adler, R. Beranek, B. Dietzek, *ChemSusChem* **2021**, *14*, 1728; i) A. J. Rieth, Y. Qin, B. C. M. Martindale, D. G. Nocera, *J. Am. Chem. Soc.* **2021**, *143*, 4646.

[3] a) A. Savateev, B. Kurpil, A. Mishchenko, G. Zhang, M. Antonietti, *Chem. Sci.* **2018**, *9*, 3584; b) H. Schlomberg, J. Kroger, G. Savasci, M. W. Terban, S. Bette, I. Moudrakovski, V. Duppel, F. Podjaski, R. Siegel, J. Senker, R. E. Dinnebier, C. Ochsenfeld, B. V. Lotsch, *Chem. Mater.* **2019**, *31*, 7478.

[4] a) I. Krivtsov, D. Mitoraj, C. Adler, M. Ilkaeva, M. Sardo, L. Mafra, C. Neumann, A. Turchanin, C. Li, B. Dietzek, R. Leiter, J. Biskupek, U. Kaiser, C. Im, B. Kirchhoff, T. Jacob, R. Beranek, *Angew. Chem., Int. Ed.* **2020**, *59*, 487; b) V. W. Lau, I. Moudrakovski, T. Botari, S. Weinberger, M. B. Mesch, V. Duppel, J. Senker, V. Blum, B. V. Lotsch, *Nat. Commun.* **2016**, *7*, 12165.

[5] a) Y. Markushyna, P. Lamagni, C. Teutloff, J. Catalano, N. Lock, G. Zhang, M. Antonietti, A. Savateev, *J. Mater. Chem. A* **2019**, *7*, 24771; b) F. Podjaski, J. Kroger, B. V. Lotsch, *Adv. Mater.* **2018**, *30*, 1705477; c) F. Podjaski, B. V. Lotsch, *Adv. Energy Mater.* **2021**, *11*, 2003049.

[6] a) H. Kasap, R. Godin, C. Jeay-Bizot, D. S. Achilleos, X. Fang, J. R. Durrant, E. Reisner, *ACS Catal.* **2018**, *8*, 6914; b) V. W. Lau, D. Klose, H. Kasap, F. Podjaski, M. C. Pignie, E. Reisner, G. Jeschke, B. V. Lotsch, *Angew. Chem., Int. Ed.* **2017**, *56*, 510; c) C. D. Windle, A. Wieczorek, L. Xiong, M. Sachs, C. Bozal-Ginesta, H. Cha, J. K. Cockcroft, J. Durrant, J. Tang, *Chem. Sci.* **2020**, *11*, 8425.

[7] a) N. Karjule, J. Barrio, L. Xing, M. Volokh, M. Shalom, *Nano Lett.* **2020**, *20*, 4618; b) H. Ou, P. Yang, L. Lin, M. Anpo, X. Wang, *Angew. Chem., Int. Ed.* **2017**, *56*, 10905; c) J. Qin, J. Barrio, G. Peng, J. Tzadikov, L. Abisdris, M. Volokh, M. Shalom, *Nat. Commun.* **2020**, *11*, 4701; d) J. Safaei, N. A. Mohamed, M. F. Mohamad Noh, M. F. Soh, N. A. Ludin, M. A. Ibrahim, W. N. Roslam Wan Isahak, M. A. Mat Teridi, *J. Mater. Chem. A* **2018**, *6*, 22346; e) J. W. Xia, N. Karjule, L. Abisdris, M. Volokh, M. Shalom, *Chem. Mater.* **2020**,

*32*, 5845; f) J. Zhang, M. Zhang, L. Lin, X. Wang, *Angew. Chem., Int. Ed.* **2015**, *54*, 6297.

[8] M. Shalom, S. Gimenez, F. Schipper, I. Herraiz-Cardona, J. Bisquert, M. Antonietti, *Angew. Chem., Int. Ed.* **2014**, *53*, 3654.

[9] J. Albero, E. M. Barea, J. Xu, I. Mora-Seró, H. Garcia, M. Shalom, *Adv. Mater. Interfaces* **2017**, *4*, 1600265.

[10] C. Adler, I. Krivtsov, D. Mitoraj, L. dos Santos-Gómez, S. García-Granda, C. Neumann, J. Kund, C. Kranz, B. Mizaikoff, A. Turchanin, R. Beranek, *ChemSusChem* **2021**, *14*, 2170.

[11] a) F. L. Formal, E. Pastor, S. D. Tilley, C. A. Mesa, S. R. Pendlebury, M. Gratzel, J. R. Durrant, *J. Am. Chem. Soc.* **2015**, *137*, 6629; b) C. A. Mesa, L. Francas, K. R. Yang, P. Garrido-Barros, E. Pastor, Y. Ma, A. Kafizas, T. E. Rosser, M. T. Mayer, E. Reisner, M. Gratzel, V. S. Batista, J. R. Durrant, *Nat. Chem.* **2020**, *12*, 82; c) E. Pastor, F. L. Formal, M. T. Mayer, S. D. Tilley, L. Francas, C. A. Mesa, M. Gratzel, J. R. Durrant, *Nat. Commun.* **2017**, *8*, 14280.

[12] a) S. Feldmann, S. Macpherson, S. P. Senanayak, M. Abdi-Jalebi, J. P. H. Rivett, G. J. Nan, G. D. Tainter, T. A. S. Doherty, K. Frohna, E. Ringe, R. H. Friend, H. Sirringhaus, M. Saliba, D. Beljonne, S. D. Stranks, F. Deschler, *Nat. Photonics* **2020**, *14*, 123; b) K. E. Hughes, K. H. Hartstein, D. R. Gamelin, *ACS Nano* **2018**, *12*, 718; c) T. Liu, D. Xiang, Y. Zheng, Y. Wang, X. Wang, L. Wang, J. He, L. Liu, W. Chen, *Adv. Mater.* **2018**, *30*, 1804470; d) A. M. Schimpf, C. E. Gunthardt, J. D. Rinehart, J. M. Mayer, D. R. Gamelin, *J. Am. Chem. Soc.* **2013**, *135*, 16569.

[13] a) B. Tan, S. R. Raga, K. J. Rietwyk, J. Lu, S. O. Fürer, J. C. Griffith, Y.-B. Cheng, U. Bach, *Nano Energy* **2021**, *82*, 105658; b) S. Elmas, W. Beelders, J. Nash, T. J. Macdonald, M. Jasieniak, H. J. Griesser, T. Nann, *RSC Adv.* **2016**, *6*, 70691.

[14] T. Berger, D. Monllor-Satoca, M. Jankulovska, T. Lana-Villarreal, R. Gomez, *ChemPhysChem* **2012**, *13*, 2824.

[15] The standard Gibbs free energy change for photoreforming of methanol to hydrogen and formaldehyde was calculated from standard Gibbs energies of formation tabulated in P. Atkins, J. de Paula, *Atkins' Physical Chemistry*, Oxford University Press, Oxford **2014**, Resource section, Table 2C.4.

[16] K. Rajeshwar, A. Vali, J. F. de Brito, M. V. Boldrin Zanoni, *ACS Energy Lett.* **2021**, *6*, 2198.

[17] L. M. Peter, *Chem. Rev.* **1990**, *90*, 753.

[18] C. A. Mesa, A. Kafizas, L. Francas, S. R. Pendlebury, E. Pastor, Y. Ma, F. L. Formal, M. T. Mayer, M. Gratzel, J. R. Durrant, *J. Am. Chem. Soc.* **2017**, *139*, 11537.

[19] B. D. Paulsen, K. Tybrandt, E. Stavrinidou, J. Rivnay, *Nat. Mater.* **2020**, *19*, 13.

[20] S. Selim, E. Pastor, M. Garcia-Tecedor, M. R. Morris, L. Francas, M. Sachs, B. Moss, S. Corby, C. A. Mesa, S. Gimenez, A. Kafizas, A. A. Bakulin, J. R. Durrant, *J. Am. Chem. Soc.* **2019**, *141*, 18791.

[21] a) M. Bledowski, L. Wang, S. Neubert, D. Mitoraj, R. Beranek, *J. Phys. Chem. C* **2014**, *118*, 18951; b) M. Bledowski, L. Wang, A. Ramakrishnan, A. Betard, O. V. Khavryuchenko, R. Beranek, *ChemPhysChem* **2012**, *13*, 3018; c) P. Longchin, D. Mitoraj, O. M. Reyes, C. Adler, N. Wetchakun, R. Beranek, *J. Phys. Energy* **2020**, *2*, 044001; d) L. Wang, D. Mitoraj, S. Turner, O. V. Khavryuchenko, T. Jacob, R. K. Hocking, R. Beranek, *ACS Catal.* **2017**, *7*, 4759.